Chemistry Faculty Research & Creative Works   Chemistry

01 Jan 2024

Perfect Polar Alignment Of Parallel Beloamphiphile Layers: Improved Structural Design Bias Realized In Ferroelectric Crystals Of The Novel "Methoxyphenyl Series Of Acetophenone Azines"

Harmeet Bhoday

Nathan Knotts

Rainer Glaser
Missouri University of Science and Technology, glaserr@mst.edu

Follow this and additional works at: https://scholarsmine.mst.edu/chem_facwork

Part of the Chemistry Commons

Recommended Citation

H. Bhoday et al., "Perfect Polar Alignment Of Parallel Beloamphiphile Layers: Improved Structural Design Bias Realized In Ferroelectric Crystals Of The Novel "Methoxyphenyl Series Of Acetophenone Azines"," *Chemistry - A European Journal*, Wiley, Jan 2024.
The definitive version is available at https://doi.org/10.1002/chem.202400182

Chemistry–A European Journal

Research Article
doi.org/10.1002/chem.202400182

Chemistry
Europe
European Chemical
Societies Publishing

www.chemeurj.org

Perfect Polar Alignment of Parallel Beloamphiphile Layers: Improved Structural Design Bias Realized in Ferroelectric Crystals of the Novel "Methoxyphenyl Series of Acetophenone Azines"

Harmeet Bhoday,[a] Nathan Knotts,[b] and Rainer Glaser*[a]

An improved design is described for ferroelectric crystals and implemented with the "methoxyphenyl series" of acetophenone azines, (MeO–Ph, Y)-azines with Y=F (**1**), Cl (**2**), Br (**3**), or I (**4**). The crystal structures of these azines exhibit polar stacking of parallel beloamphiphile monolayers (PBAMs). Azines **1**, **3**, and **4** form true racemates whereas chloroazine **2** crystallizes as a kryptoracemate. Azines **1–4** are helical because of the N–N bond conformation. In true racemates the molecules of opposite helicity (*M* and *P*) are enantiomers **A**(*M*) and **A***(*P*) while in kryptoracemates they are diastereomers **A**(*M*) and **B***(*P*). The stacking mode of PBAMs is influenced by halogen bonding, with **2–4** showcasing a kink due to directional *inter*layer halogen bonding, whereas fluoroazine **1** demonstrates ideal polar stacking by avoiding it. Notably, (MeO–Ph, Y)-azines display a stronger bias for dipole parallel alignment, attributed to the linearity of the biphenyl moiety as compared to the phenoxy series of (PhO, Y)-azines with their non-linear Ph–O–Ph moiety. The crystals of **1–4** all feature planar biphenyls and this synthon facilitates their crystallization through potent triple T-contacts and enhances their nonlinear optical (NLO) performance by increasing conjugation length and affecting favorable chromophore conformations in the solids.

Introduction

Polar donor-acceptor substituted organic molecular crystals are desirable for their applications in the fields of nonlinear optics (NLO), optoelectronics, terahertz generation, electro-optics, photovoltaics, fluorescence, polymorphism, and crystal engineering.[1–8] Our focus is on the fabrication of ferroelectric organic molecular crystals with high second-order NLO effects. For organic crystals to exhibit second-order NLO effects they must crystallize in a non-centrosymmetric space group. Most polar molecules crystallize in such a way as to compensate dipole moments rendering their crystals essentially non-polar. Large-scale polar order is a very rare phenomenon and there are only a few serendipitous cases with significant dipole parallel alignment. Side-by-side molecular dipoles prefer an antiparallel arrangement for electrostatic reasons while collinear dipoles adopt parallel alignment, and therefore non-polar crystals are formed. Large scale polar order in organic crystals was thought to be unachievable for a long time and it presents a grand challenge. However, we have shown theoretically that parallel aligned dipole lattices may occur as local minima.[9] Thus there is a chance to obtain polar crystals by rational design.

The concepts guiding the fabrication of these ferroelectric materials have been described[10–12] and they are based on amphiphile monolayers (AM). Amphiphiles (Greek, *amphibios*) are "living a double life" by combination of a polar and water-soluble head group and a nonpolar and water-insoluble alkyl chain. Idioteloamphiphiles contain two polar head groups of the same kind (Greek, *idios*) at the ends (Greek, *telos*) of a nonpolar chain. Beloamphiphiles contain two polar head groups of different kinds and the prefix *belo* (Greek, *belos*, arrow) reflects their polarity. Our focus was with unsymmetrical donor-acceptor substituted azines D–Ph–(R)C=N–N=C(R)–Ph–A (Scheme 1, left). The original idea was to design molecules that would encourage strong lateral attractive interactions between side-by-side molecules to build parallel beloamphiphile monolayers (PBAMs). The acetophenone azines include two phenyl rings which were expected to engage in arene-arene interactions between neighboring molecules. This strategy certainly encouraged the formation of beloamphiphile monolayers (BAMs) but the realization of PBAMs also relied on the expectation that arene-arene interactions between like-substituted arenes (D–Ph//D–Ph and A–Ph//A–Ph) exceed arene-arene interactions between differently substituted arenes (D–Ph// A–Ph). Therefore, it became our goal not just to encourage BAM formation but to deliberately discourage antiparallel alignment between neighbors within a BAM. This strategy was first implemented with the phenoxy series of acetophenone azines Ph–O$_{para}$–Ph–(Me)C=N–N=C(Me)–Ph–Y$_{para}$ (Scheme 1,

[a] H. Bhoday, Dr. R. Glaser
Department of Chemistry
Missouri University of science and Technology
Rolla, MO, 65409 USA
E-mail: glaserr@umsystem.edu

[b] Dr. N. Knotts
Department of Chemistry
University of Missouri
Columbia, MO, 65211 USA

Supporting information for this article is available on the WWW under https://doi.org/10.1002/chem.202400182
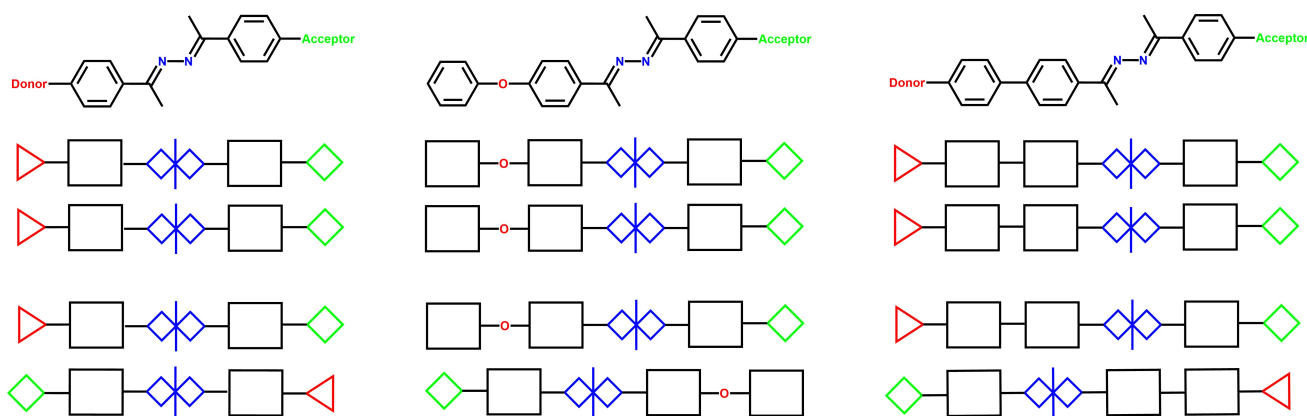
Scheme 1. BAM design to achieve polar stacking of parallel beloamphiphile monolayers (PBAMs) of (RO, Y)-azines (left), (PhO, Y)-azines (center), and (RO–Ph, Y)-azines (right). Rows, top to bottom: Molecular structures schematic descriptions of azine design, and their lateral interactions upon parallel and antiparallel alignment.

center), which can only realize three arene-arene interactions if side-by-side neighbors are parallel aligned.

Azines RO_{para}–Ph–(Me)C=N–N=C(Me)–Ph–Y_{para} stand out because we have been able to fabricate crystals with perfect dipole alignment in several series of acetophenone azines. Initial success came with the methoxy series (RO=MeO) with Y=Cl,[13] Br,[14] I,[15] and we have since realized several materials in the phenoxy series (RO=PhO)[16,17] with Y=F,[18] Cl,[19] Br,[20] and I[21] and the decyloxy series (RO=DecO)[22] with Y=F,[23] Cl,[24] and Br.[25]

However, there also are several examples of antiparallel alignment of next neighbors in antiparallel beloamphiphile monolayers (APBAMs). For the generic (X, Y)-acetophenone azines the list of antiparallel alignment in crystal structures includes the (EtO, Cl)-azine,[26] (EtO, Br)-azine,[27] (PrO, I)-azine,[28] and (i-PrO, Br)-azine.[29] Even though the phenoxy and decyloxy series both have additional incentives for parallel alignment built into the azine structures, there are examples in both series that do feature antiparallel alignment and these include the crystal structures of (PhO, NO$_2$)-acetophenone azine[30] and (DecO, NO$_2$)-acetophenone azine.[31]

Even in the case of perfect PBAM construction, we have learned that polar stacking of PBAMs is not assured. We have recently discussed polymorphs of (PhO, F)-acetophenone azine which exemplify polar and non-polar stacking of perfectly parallel aligned monolayers (PBAMs).[17] We are aware that the imine Bu–Ph–N=CH–Ph–Ph (PB4 A, (E)–N-(biphenyl-4-ylmethylene)-4-butylaniline) presents one other case of non-polar stacking of PBAMs,[32] and in this case, a polymorph with polar stacking has not yet been discovered.

While our primary interest always has been with *unsymmetrical* azines, we have also studied intensively the *symmetrical* azines to learn about the intermolecular interactions in azine crystals.[33–35] A special case of the (PhO, F)-azine led us to study symmetrical (Y, Y)-azines.[36]

Here we report on the new "methoxyphenyl series of acetophenone azines", the (MeO–Ph, Y)-azines, that is, the (E,E)-4'-(4"-methoxyphenyl)acetophenone 4-haloacetophenone azines MeO_{para}–Ph–Ph–(Me)C=N–N=C(Me)–Ph–Y_{para} (Scheme 1,

right). These NLO chromophores present an improved variation of the phenoxy series by avoidance of the non-linearity of the Ph–O–Ph moiety. Strictly speaking, the molecules of this new series are mixed azines formed by combination of one halogen-substituted acetophenone, O=C(Me)–Ph–Y_{para} and one methoxy-substituted 4-acetylbiphenyl, MeO_{para}–Ph–Ph–(Me)C=O. We synthesized the (MeO–Ph, Y)-azines with Y=F (**1**),[37] Cl (**2**),[38] Br (**3**),[39] and I (**4**).[40] Single-crystals were grown, and single-crystal X-ray analysis shows perfectly parallel aligned azines in the crystal structures of **1**–**4**. The methoxyphenyl azines crystallize with layered structures containing perfectly parallel aligned azines in their PBAMs and all realize polar PBAM stacking. Characteristics of their lattice architectures are described with focus on triple T-contacts within the PBAMs and the *inter*layer interactions between PBAMs. Hirshfeld 2-D fingerprint plots were generated, and they allow for the quick distinction between PBAM morphologies and provide insights about the relation between halogen bonding and PBAM stacking modes. The complete conformational space of azines **1**–**4** was explored (Scheme 2) and revealed crystal packing effects on the molecular structures of the azines. Optical performance data were computed (dipole moments and first-
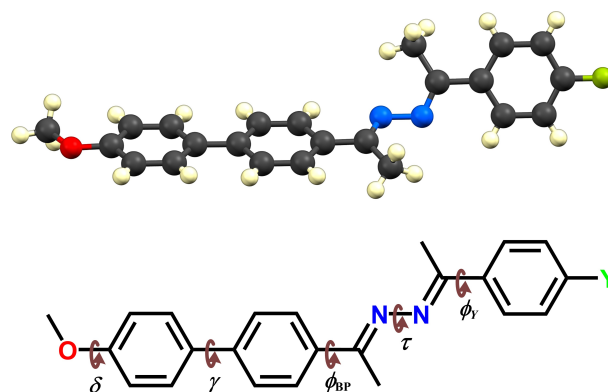
Scheme 2. Chemical structure of (MeO–Ph, Y)-azine. Definition of nomenclature for important torsion angles governing molecular conformation.

Chemistry–A European Journal

Research Article
doi.org/10.1002/chem.202400182

Chemistry Europe
European Chemical
Societies Publishing

order hyperpolarizabilities) and are discussed in comparison to the phenoxy and methoxy series.

Results and Discussion

Crystal Structures of (MeO–Ph, Y)-Azines

All four (MeO–Ph, Y)-azines crystallize in ferroelectric space groups. (MeO–Ph, F)-azine crystallizes in monoclinic space group Pc, (MeO–Ph, Cl)-azine crystallizes in monoclinic space group P2$_1$ and both the (MeO–Ph, Br)- and (MeO–Ph, I)-azine crystallize in orthorhombic space group Pna2$_1$. The reflections for the azine where Y$=$F were recorded at 293 K while that for the azines where Y$=$Cl, Br, and I were recorded at 173 K. Crystal structure details of the four azines are listed in Table 1. It is worth noting that there are two unique molecules (Z$'=$2) in the unit cell of (MeO–Ph, Cl)-azine while the other azines contain only one (Z$'=$1) unique molecule in their unit cells. ORTEP diagrams of **1**–**4** are shown in Figure 1 (ESI†) and we begin with a brief discussion of the molecular topology with focus on the conformation of the biphenyl moiety (γ) and the azine twist (τ).

As in the crystal structure of biphenyl itself,[41] the biphenyl moieties in **1**–**4** are essentially coplanar in all four crystals with $\gamma \approx 0$. This structural feature is remarkable because free biphenyls are well known for featuring significant γ twist with $\gamma \approx 43°$ for biphenyl in the gas phase.[42,43] One might expect that donor-acceptor substitution of biphenyls might lead to a coplanar arenes to improve conjugation. However, in our own studies of 4′-acetyl-4-methoxybiphenyl we found the molecule to be twisted with $\gamma = 42.9°$ in the gas phase and a near coplanar biphenyl with $\gamma = 2.6°$ occurred only in the crystal structure.[44]

The azines show the usual azine twist $133° < |\tau| < 143°$ and the azine and the phenyl twists (ϕ_{BP} and ϕ_Y range) cooperate to maximize the angle between the best planes of the biphenyl

moiety and the third arene. For the C$=$N–N$=$C conformation, the helicity is referred to as *P* if a clockwise rotation is required about the N–N bond for the proximate C$=$N bond ($\tau > 0$) to eclipse the distal C$=$N bond and it is *M* if a counter-clockwise rotation is required ($\tau < 0$). The unique molecules are shown with *M*-helicity in Figure 1 (ESI†) for Y$=$F, Br, and I. For every molecule with *M*-helicity the crystal contains an enantiomer with *P*-helicity, and these crystals are true racemates. The situation is more interesting for Y$=$Cl because the unit cell contains two unique molecules **A** and **B*** with *M*- and *P*-helicity, respectively. We refer to the independent molecules as **A** and **B*** (instead of **A** and **B**) to emphasize their different helicities (*M* unstarred, *P* starred). Since the **A** and **B*** molecules are structurally different, they are not enantiomers, but they are *diastereomers* instead, and they form a kryptoracemic crystal. Fabian and Brock estimated that organic kryptoracemates occur in only about 0.1% of racemic crystals.[45] The crystal structures show that a given azine helicity is strictly correlated with the helicities of the phenyl twists (azine twist *M*-helicity is always associated with phenyl twist *P*-helicities and *vice versa*), and the specification of the azine twist helicity therefore fully describes the molecular stereochemistry.

Parallel Beloamphiphile Monolayer (PBAM) Architecture

The crystal structure analysis shows the polar stacking of perfectly parallel aligned beloamphiphile monolayers (PBAMs) for **1**–**4**. The PBAM of **1** is shown in Figure 1 and compared to the PBAM of (PhO, F)-azine.

There is some lateral offset between neighboring azines which we describe by the leaning angle λ, which is enclosed between the long axis of each molecule and the normal vector of the layer surface. The direction of the long axis of each molecule is defined by the azine N–N bond direction. The leaning angles in **1**–**4** are $\lambda(F) = 25.46°$, $\lambda(Cl) = 26.06°$, $\lambda(Br) = 25.47°$, and $\lambda(I) = 25.66°$, respectively. These leaning angles are very similar to the respective values measured for the methoxy and the phenoxy series.[16]

As anticipated, neighboring molecules in the PBAMs of the (MeO–Ph, Y)-azines engage in triple T-contacts. However, the specific characteristics of the triple T-contacts differ significantly between the (MeO–Ph, Y)-azines and the (PhO, Y)-azines and this is exemplified in Figure 1. We recently described the triple T-contact in the (PhO, Y)-azines as (ef|fe|ef) arene-arene
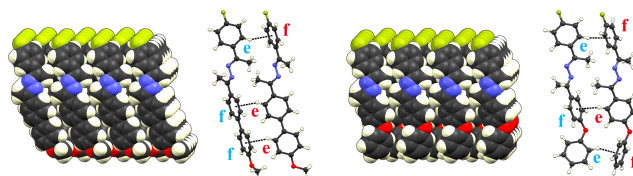
Table 1. Crystallographic parameters of (MeO–Ph, Y)-azines **1**–**4**.				
	1	**2**	**3**	**4**
Crys. Sys.	Mono-clinic	Mono-clinic	Ortho-rhombic	Ortho-rhombic
Space gr.	Pc	P2$_1$	Pna2$_1$	Pna2$_1$
a/Å	19.4309(17)	6.2587(4)	6.3923(6)	6.3980(3)
b/Å	7.2170(6)	39.240(3)	7.2363(6)	7.2597(3)
c/Å	6.5163(6)	7.6710(5)	40.927(4)	41.4797(19)
α/°	90	90	90	90
β/°	98.795(2)	95.941(2)	90	90
γ/°	90	90	90	90
V/Å^3	903.05(14)	1818.7(7)	1893.2(3)	1926.63(15)
Z/Z′	2/1	4/2	4/1	4/1
T/K	293(2)	173(2)	173(2)	173(2)
R1	0.0515	0.0443	0.0590	0.0265
w*R2* (all)	0.1484	0.1006	0.1539	0.0624
GooF	0.977	1.027	1.185	1.062

Figure 1. Monolayer architecture in the crystals of (MeO–Ph, F)-azine, 1 (left) and the corresponding (PhO, F)-azine (right). Space-filling presentations are shown of the PBAMs, and the leaning angles are λ(MeO–Ph, F)$=$25.46° and λ(PhO, F)$=$25.80°. The ball-and-stick models show triple T-contacts in one pair of molecules.

contacts, that is, one molecule engages two arene edges (e) and one arene face (f) while the other engages one edge and two faces. In all (MeO–Ph, Y)-azines, the biphenyl moiety is essentially planar and requires the biphenyl moiety to engage as a double edge synthon or a double face synthon. Because of the azine twist, the third arene will always engage in the opposite manner relative to the biphenyl arenes. For example, the (MeO–Ph, F)-azines in the pair shown in Figure 1 engage as (f|f|e) and (e|e|f) molecules and result in one (fe|fe||ef) pair interaction. Each (MeO–Ph, F)-azine interacts with the four next neighbors and forms two (fe|fe||ef) and two (ef|ef||fe) interactions.

Polar Stacking of PBAMs

Polar stacking of the PBAMs is realized for **1–4** and space-filling models of three PBAMs are shown in Figure 2. Polar stacking means that the halogen surface of a PBAM is placed close to the methoxy surface of the next PBAM. Perfect polar stacking occurs in crystals of fluoroazine **1**, that is, the orientations of the long axes of every molecule in every layer are exactly the same. The three other azines afford near-perfect polar stacking, that is, the dipole directions in adjacent PBAMs are near-perfectly aligned and the kink angle κ describes the degree of their alignment. The kink angle κ is defined as the angle enclosed between the long axes of molecules in adjacent PBAMs.

Figure 2 shows "flat" layer architectures for Y = F, Br, and I while the crystal structure of the chloro compound adopts the "AB-kick/flat" layer architecture.[36] In the flat architecture, the longitudinal offset between the neighboring molecules goes in the same direction, whereas the direction of the longitudinal offset between neighboring molecules alternates in the AB-kick/flat layer architecture. This alternative layer architecture leads to different pair geometries, different *intra-* and *inter*layer interaction topologies, and some aspects of *inter*layer interactions are illustrated in Figure 3.

The *inter*layer architectures of the (MeO–Ph, Br)-azine, **3** and of the (MeO–Ph, I)-azine, **4** show clear evidence of halogen
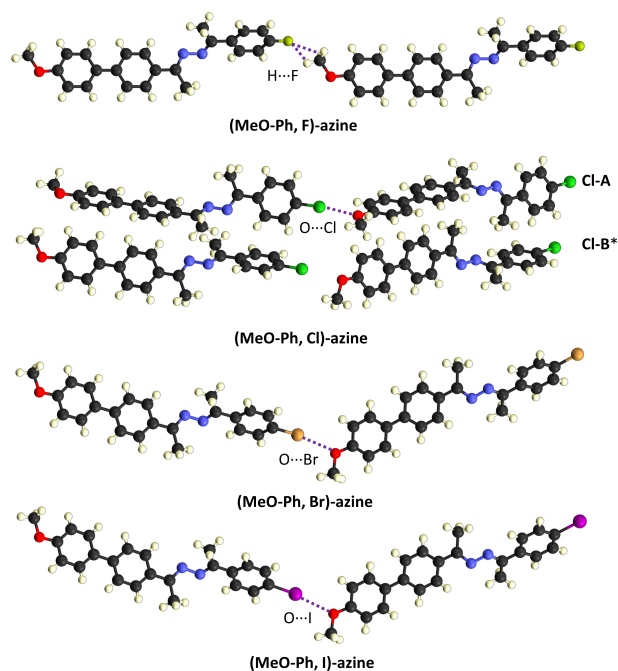

Figure 3. Stacking mode and *inter*layer contacts. Halogen bonding causes the kinks of **2–4** because this mode of PBAM stacking ensures proper directionality of the C–Y⋯O interaction. The stacking of fluoroazine **1** is not constrained by directional preferences of halogen bonding.

bonding between the methoxy-O and the haloarenes. These interactions are characterized by the d(O⋯Y) distance (Br: 3.06 Å, I: 3.14 Å) and the $\angle$(C–Y⋯O) angle (Br: 169.7°, I: 171.8°).

The *inter*layer interaction in (MeO–Ph, F)-azine, **1** is entirely different in that halogen bonding does not play a role (d(O⋯F) = 3.2 Å, $\angle$(C–F⋯O) = 99.2°). The fluoroazine interacts with its *inter*layer neighbor of the same helicity via the fluorine and the methoxy-Me (d(H⋯F) = 2.58 Å, $\angle$(C–H⋯F) = 118.2°).

The main *inter*layer contacts of chloroazine **2-A** are similar to situations with the bromo- and iodo-azines. The chlorine of **A** engages in halogen bonding with its primary **A** *inter*layer neighbor (d(O⋯Cl) = 2.90 Å, $\angle$(C–Cl⋯O) = 175.6°). The main *inter*-
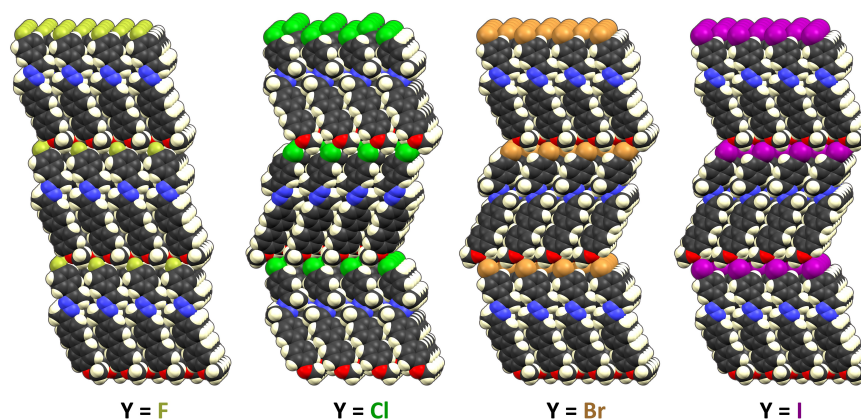

Figure 2. Space-filling trilayer presentations show polar stacking of PBAMs in crystals of (MeO–Ph, Y)-acetophenone azines, from left: Y = F, Cl, Br, I. Perfect parallel stacking occurs in crystals of (MeO–Ph, F)-acetophenone azine and the other halogens afford near-perfect parallel stacking (note the zigzag pattern). The kink angles are κ(F) = 0°, κ(Cl) = 127.88°, κ(Br) = 129.06° and κ(I) = 128.68°.

layer contacts of **2-B*** are very different because the **B*** molecule does *not* engage in halogen bonding. The distance between chlorine and the proximate methoxy-O is 3.31 Å and out of the range of $d(\text{O}\cdots\text{Cl})$ halogen bonds.

The topologies of the *inter*layer interactions of the **A**(*M*) and **B***(*P*) molecules differ drastically. It is for this reason that the chloroazines with *M*- and *P*-helicity are *coordination isomers.* While we have focused on the description of the helicity using the azine twist angle τ, recognizing **A**(*M*) and **B***(*P*) as coordination isomers begs the question about other noticeable structural differences between the two molecules. This comparison was made with reference to computational studies of the conformations of (MeO–Ph, Y)-azines.

Hirshfeld Surface Analysis

In our recent study of the lattice architectures of a large series of symmetrical acetophenone azines,[36] we discovered that the N⋯H Hirshfeld fingerprint (HFP) plots allow for an easily accessible evaluation of the idioteloamphiphile monolayer (IAM) morphology without any structural analysis. We showed that flat IAMs exhibit flower-like patterns with four petals while kick/flat IAMs manifest themselves in curtain-like patterns. This relation between IAM morphology and N⋯H fingerprint plot patterns only depends on relative position of azines and arenes independent of the type of (X, Y)-substitution pattern. Hence, the relation observed for the symmetrical azines is expected to hold for PBAMs of unsymmetrical azines. Indeed Figure 2 (ESI†) demonstrates that the flat PBAMs of (MeO–Ph, Y)-azines **1**, **3**, and **4** show well defined four petal flower patterns whereas the kick/flat PBAM in chloroazine **2** shows a curtain pattern.

The structural evidence for halogen bonding in **3** and **4** is corroborated by the HFP plots in Figure 4. Sharp spikes indicate directional short-range bonding between the methoxy-O atoms and the haloarenes' hydrogen atoms with distances shorter than the sum of their van der Waals radii. These contacts also appear as red spots on the Hirshfeld surfaces (Figure 3, ESI†). The Hirshfeld analysis corroborates the conceptual difference of
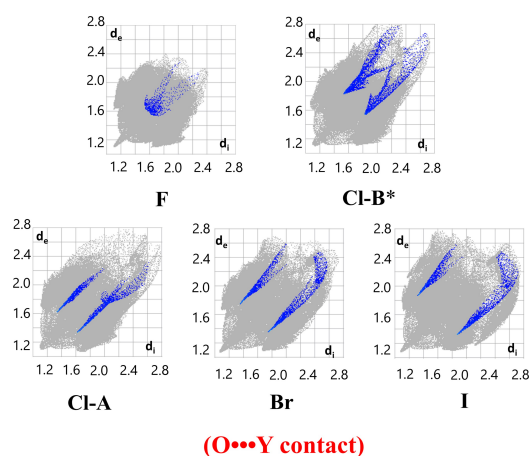
the lattice architecture of fluoroazine **1**. Halogen bonding plays no role: O⋯F contacts are few in numbers (0.7%), all are non-directional (no spikes), and distances exceed vdW sums. The H⋯F *inter*layer bonding mode is manifested by the red spot on the Hirshfeld surface (Figure 3, ESI†). This type of $\text{H}_{\text{MeO}}\cdots\text{F}$ contact is unique to fluoroazine **1**.

The O⋯Cl HFP plot for **2-A** greatly resembles the O⋯Y plots of **3** and **4** and clearly each **2-A** molecule engages in a strong halogen bond ($d_i + d_e \approx 2.9$ Å). In sharp contrast, the respective O⋯Cl HFP plot for **2-B*** (Figure 4) shows no evidence for halogen bonding; the spikes are less sharp, and contacts are much longer ($d_i + d_e > 3.3$ Å).

Molecular Structure and Conformations of (MeO–Ph, Y)-Azines

The shapes of the (MeO–Ph, Y)-azines are characterized by five dihedral angles (Scheme 2) and their values are listed in Table 2. Six sets of calculations were performed at the APFD/6-311G* level for each unique molecule using Gaussian 16.[46] The azine molecules in the crystals are referred to as the **a** molecules, all **Xa** structures feature essentially planar biphenyl moieties, and we determined their single point energies with the crystal coordinates. Hydrogen positions are notoriously ill estimated, and we optimized **XaH** structures with the positions of all heavy atoms retained as in the crystal structure but with hydrogen positions optimized. Furthermore, we optimized **Xb** structures with the single constraint that the biphenyl twist angle γ was fixed to the value measured in the crystal structures. The (MeO–Ph, Cl)-azine **2** features two independent molecules **A** and **B*** in its crystal structure and we computed the constrained structures **2aH–A** and **2b-A** with *M*-helicity as well as **2aH-B*** and **2b-B*** with *P*-helicity. The relative energies of the **XaH** and **Xb** structures will allow for an estimate of the energy associated with the adoption of the crystal structure conformation relative to the free minima.

The free molecules **X** can adopt eight stereoisomers that group into four pairs of enantiomers, and the unique *M*-enantiomers are shown in Figure 4 (ESI†) for the azines **1–4**. The supplementary information also contains Cartesian coordinates of the optimized structures. The description of their conformations requires well thought out conventions regarding the definition of the twist angles. The phenyl twist angles $\phi_Y = \angle(\text{C}_o{}^*\text{–C}_i\text{–C=N})$ and $\phi_{BP} = \angle(\text{C}_o{}^*\text{–C}_i\text{–C=N})$ always refer to the ortho-C that is closest to an azine-N and those carbons are starred in Figure 5. The conformation of the methoxy group is
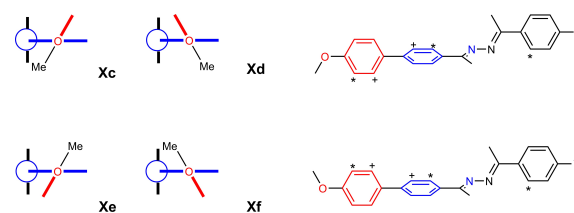

Figure 4. Hirshfeld 2-D fingerprint plots resolved into *inter*layer O⋯Y in the crystals of **1–4**.

Figure 5. Possible stereoisomers of (MeO–Ph, Y)-azines.

Chemistry–A European Journal

Research Article
doi.org/10.1002/chem.202400182

Chemistry Europe
European Chemical
Societies Publishing

Table 2. Dihedral angles of (MeO−Ph, Y)-azines in crystals and gas phase.[a–c]

Molecule		τ	ϕ_Y	ϕ_{BP}	γ	δ	E_{rel}
(MeO−Ph, F)	1a	−142.9	11.8	10.1	2.6	2.1	
	1aH	−142.9	11.8	10.1	2.6	2.1	3.961
	1b	−135.2	15.3	14.8	2.6	−0.1	2.219
	1c	−135.1	15.2	14.8	39.6	−0.5	0.003
	1d	−134.3	15.4	15.5	140.4	0.4	0.011
	1e	−135.3	15.1	14.9	−140.2	−0.4	0.029
	1f	−134.5	15.3	15.6	−39.6	0.4	0.000
(MeO−Ph, Cl)	2a-A	−133.2	1.7	12.2	0.1	−3.2	
	2aH-A	−133.2	1.7	12.2	0.1	−3.2	4.703
	2b-A	−134.2	15.0	13.7	0.1	0.0	2.251
	2a-B*	134.6	−13.3	−2.8	−1.2	−1.8	
	2aH-B*	134.6	−13.3	−2.8	−1.2	−1.8	4.482
	2b-B*	134.4	−15.0	−13.7	−1.2	0.0	2.306
	2c	−134.1	15.3	14.6	39.6	−0.5	0.003
	2d	−133.2	15.3	15.5	140.4	0.0	0.009
	2e	−134.1	15.3	14.6	−140.2	−0.5	0.029
	2f	−133.2	15.3	15.5	−39.5	0.5	0.000
(MeO−Ph, Br)	3a	−141.3	8.5	10.8	−0.2	0.3	
	3aH	−141.3	8.5	10.8	−0.2	0.3	5.070
	3b	−134.3	15.1	13.8	−0.2	0.0	2.353
	3c	−133.9	15.3	14.9	39.6	−0.5	0.003
	3d	−133.1	15.5	15.5	140.4	0.4	0.009
	3e	−134.2	15.2	14.9	−140.2	−0.4	0.031
	3f	−133.4	15.4	15.6	−39.5	0.5	0.000
(MeO−Ph, I)	4a	−142.1	8.0	12.4	−0.3	−1.2	
	4aH	−142.1	8.0	12.4	−0.3	−1.2	4.207
	4b	−133.9	15.2	14.1	−0.3	0.0	2.300
	4c	−133.6	15.2	14.7	39.6	−0.5	0.003
	4d	−132.8	15.6	15.5	140.4	0.3	0.008
	4e	−133.9	15.2	15.0	−140.2	−0.4	0.031
	4f	−133.1	15.4	15.6	−39.5	0.5	0.000

[a] $\tau = \angle(C{=}N{-}N{=}C)$, ϕ_Y and ϕ_{BP} employ the *syn* C_o atom, $\phi_Y = \angle(C_o*{-}C_i{-}C{=}N)$, $\phi_{BP} = \angle(C_o*{-}C_i{-}C{=}N)$, $\gamma = \angle(C^+{-}C{-}C{-}C^+)$, $\delta = \angle(H_3C{-}O{-}C_i{-}C_o*)$, see Figure 5. [b] **Xa** describes the crystal structure. **Xb** computed with γ (**Xa**). Minimum **Xc** with $\gamma > 0$ and minimum **Xd** with $\gamma < 0$. [c] Energy E_{rel} in kcal/mol relative to most stable minimum.

described by $\delta = \angle(H_3C{-}O{-}C_i{-}C_o*)$ and δ will always be determined with the ortho-C that is closest to the methyl group, which is starred in Figure 5. The carbons marked by superscript "+" share a common edge with the starred carbons, and with these definitions of the two C+-carbons in the biphenyl moiety, we can now describe the biphenyl twist unambiguously with the dihedral angle $\gamma = \angle(C^+{-}C{-}C{-}C^+)$. The data in Table 2 shows that the structures **Xc–Xf** for a given **X** feature essentially the same azine twist angles τ and phenyl twist angles ϕ_Y and ϕ_{BP} whose signs are inversely correlated with the τ values. Structures **Xc–Xf** differ only in their γ angles and all of them clearly show non-planar biphenyls.

The last column of Table 2 lists relative energies E_{rel} in kcal/mol with reference to the most stable minimum. The conformations **Xc–Xf** are essentially isoenergetic. The relative energies of the **Xb** structures provide a good estimate for the barrier of rotation around the Ph–Ph bond through the planar structure and the calculations show essentially free rotation in the gas phase with relative energies below 3 kcal/mol. The relative energies of the **XaH** structures are most significant in the present context because they inform about the stress associated with the molecular distortions in the crystals to optimize crystal lattice energies. These distortion energies depend on the nature of Y, they fall in the range of 4–5 kcal/

Chem. Eur. J. **2024**, e202400182 (6 of 10)

© 2024 Wiley-VCH GmbH

Chemistry–A European Journal

Research Article
doi.org/10.1002/chem.202400182

Chemistry
Europe

European Chemical
Societies Publishing

mol and provide an important reference for the discussion of intermolecular bonding in the crystals.

Computed Performance Data

To study the structure-function relationship of the donor-acceptor substituted optical materials, we computed molecular dipole moments μ_m, first-order hyperpolarizabilities β_o, and molecular volumes V_{vdW} for the methoxy, phenoxy, and methoxyphenyl series of azines with Y = F, Cl, Br, and I at the APFD/6-311G* level as implemented in Gaussian 16 and the results are summarized in Table 3 together with the benchmark data for para-nitroaniline (PNA).[16]

The data for PNA and the methoxy and phenoxy azines were computed based on the optimized free molecules. The methoxyphenyl azines were studied in more detail and performance data were computed for the four conformations **Xc–Xf** as well as the constrained structures **XaH** and **Xb** with their near coplanar biphenyl moieties.

The replacement of the methoxy- or phenoxy-substituted acetophenone, RO_{para}–Ph–(Me)C=O by the methoxy-substituted 4-acetylbiphenyl, MeO_{para}–Ph–Ph–(Me)C=O drastically changes the hyperpolarizability of the free molecule (Figure 6). The β_0

Table 3. Computed dipole moments and first-order hyperpolarizabilities of (PhO, Y)-, (MeO, Y)- and (MeO–Ph, Y)-azines.

Azine		μ_m [a]	β_o [b]	μ_m/V_{vdW} [c]	β_o/V_{vdW} [d]
PNA		7.2152	10.632	61.0919	90.022
(MeO, F)		2.8952	15.269	10.6506	38.538
(PhO, F)		2.7779	15.045	7.9878	43.261
(MeO–Ph, F)	1aH	3.2434	46.116	9.4164	133.886
	1b	3.1002	42.411	9.0007	123.128
	1c	2.7275	32.894	7.9184	95.498
	1d	3.4113	30.333	9.9036	88.064
	1e	3.9072	32.876	11.3435	95.446
	1f	3.3332	30.344	9.6770	88.096
(MeO, Cl)		3.5252	18.441	12.5462	65.631
(PhO, Cl)		3.3609	18.509	9.4166	51.859
(MeO–Ph, Cl)	2aH-A	3.8591	46.009	10.9140	130.121
	2aH-B*	3.7198	46.837	10.5202	132.462
	2b-A	3.7850	49.363	10.7046	139.606
	2b-B*	3.7674	48.968	10.6547	138.488
	2c	3.4079	38.552	9.6379	109.032
	2d	4.0401	35.375	11.4261	100.046
	2e	4.4858	38.471	12.6865	108.803
	2f	3.9241	35.429	11.0980	100.198
(MeO, Br)		3.4856	18.053	12.2280	63.333
(PhO, Br)		3.3343	17.978	9.2367	49.803
(MeO–Ph, Br)	3aH	3.8000	52.783	10.6246	147.578
	3b	3.7627	49.532	10.5203	138.488
	3c	3.3671	38.218	9.4142	106.856
	3d	4.0092	34.950	11.2094	97.718
	3e	4.4528	38.201	12.4497	106.807
	3f	3.8841	35.040	10.8598	97.971
(MeO, I)		3.5960	19.166	12.3555	65.853
(PhO, I)		3.4377	18.737	9.3676	51.058
(MeO–Ph, I)	4aH	3.8583	59.435	10.6099	163.437
	4b	3.8864	51.926	10.6871	142.789
	4c	3.4821	39.588	9.5754	108.861
	4d	4.1189	36.169	11.3264	99.461
	4e	4.5524	39.461	12.5185	109.007
	4f	3.9835	36.277	10.9540	99.757

[a] In Debye. [b] In 10^{-30} esu. [c] In mDebye/Å^3. [d] In 10^{-33} esu/Å^3.

Chemistry–A European Journal

Research Article
doi.org/10.1002/chem.202400182

**Chemistry
Europe**
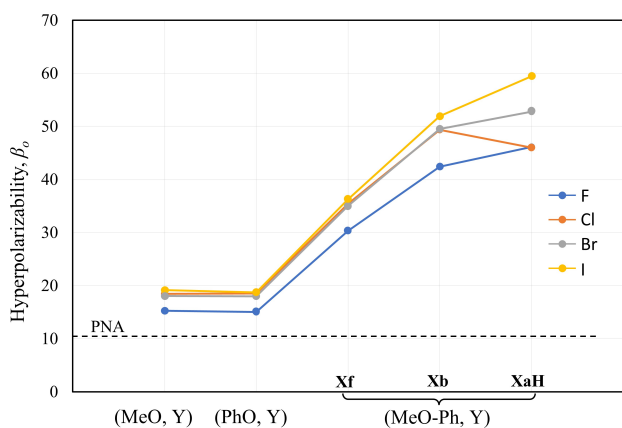European Chemical
Societies Publishing

Figure 6. First-order hyperpolarizabilities of azines and dependence on conformation in the crystals.

values of the free molecules **Xf** are essentially doubled compared to the (MeO, Y)- and (PhO, Y)-azines and trice the value of PNA. While both the (PhO, Y)- and the (MeO–Ph, Y)-azines feature improved PBAM stabilities because of triple T-contacts, the (MeO–Ph, Y)-azines also improve the conjugation length and lead to greatly improved β_0 values.

Interestingly, the calculations show that the constraints on conformations imposed by the crystal structures greatly reinforce the optical performance of the materials. While the free molecules **Xf** feature twisted biphenyls, in the crystals the molecular structures **XaH** allow for extended conjugation across the biphenyl moiety and result in an additional boost of the β_0 values by $(20\pm5)\cdot10^{-30}$ esu. For (MeO–Ph, Y)-azines with flat PBAMs, this crystal lattice related performance enhancement amounts to $15.72\cdot10^{-30}$ esu for F, $17.74\cdot10^{-30}$ esu for Br, and $23.15\cdot10^{-30}$ esu for I. The calculation of the **Xb** molecules provide evidence that most of the enhancement in going from **Xf** to **XaH** is due to forcing the planar biphenyl conformations. The crystal structure of chloroazine **2** also constraints the biphenyl moiety to near planarity, but the kick/flat architecture causes azine twist angles that are about 10° lower in the crystals. Nevertheless, the crystal lattice related performance enhancement for chloroazine **2** remains significant with $10.58\cdot10^{-30}$ esu.

Conclusions

We have described the successful synthesis of four representatives of the new "methoxyphenyl series" of acetophenone azines, (MeO–Ph, Y)-azines for short with Y = F (**1**), Cl (**2**), Br (**3**), and I (**4**). The crystal structures of these four azines feature polar stacking of parallel beloamphiphile monolayers.

The crystals of **1**, **3**, and **4** are true racemates. Crystals of the chloro compound **2** are conceptually different and present a special case of a kryptoracemate. Interaction inventory analysis shows that the independent molecules **A** and **B*** are coordination isomers, and hence the *M*- and *P*-azines must be diastereomers because they experience different intermolecular

interactions.[47] We continue to search for potential polymorphs of the discussed kryptoracemate (**A** and **B***) of chloroazine **2**, namely the enantiomeric kryptoracemate (**A*** and **B**) and the true racemate (**A** and **A***). Of course, one may also expect to find kryptoracemate polymorphs of **1**, **3**, and **4**. Landscape analyses[48] suggest that a polymorph of (MeO–BP, Cl)-azine may crystallize as a true racemate while none of the other (MeO–BP, Y)-azines has any propensity to crystallize as kryptoracemate.

The avoidance of the non-linearity associated with the Ph−O−Ph moieties in the (PhO, Y)-azines affords superior triple T-contacts between side-by-side azines and higher PBAM stabilities. As a direct consequence we observed significantly faster crystallization of the materials of the methoxyphenyl series.

It is important to note that to date we have never observed any polymorphs of (MeO–Ph, Y)-azines with antiferroelectric lattices. These NLO chromophores do have the expected and desired strong inherent bias for side-by-side dipole parallel alignment; there is a clear incentive for a biphenyl moiety to engage in lateral interactions with another biphenyl moiety rather than a biphenyl moiety engaging in lateral interactions with a phenyl-azine moiety.

The analyses of the (MeO–Ph, Y)-azines show that the mode of PBAM stacking is affected by halogen bonding. Replacements of the methoxy groups by larger alkoxy groups in (RO–Ph, Y)-azines might be a promising strategy to achieve ideal polar stacking and perfect parallel dipole alignment. Of course, the crystal structure of (MeO–Ph, F)-azine demonstrates that perfect polar stacking can be achieved by halogen bonding avoidance. We attribute this desirable feature to the absence of O⋯F halogen bonding as evidenced by the sum of their vdW radii. The *inter*layer interaction occurs via the fluorine and methoxy-Me groups and this unique H_{MeO}⋯F bonding mode is fully compatible with the electrostatically most stabilizing PBAM stacking.

At the outset of the present studies our focus was on the improvement of stable ferroelectric lattices and this goal was fully met. Beyond the achievement of this immediate crystal engineering goal, we were delighted to discover that the methoxyphenyl chromophore affords much better NLO performance compared to the methoxy and phenoxy series. The biphenyl moiety increases the conjugation length and more than doubles the hyperpolarizabilities β_o even with non-planar biphenyl geometries (**Xf**). Moreover, the crystal lattice architectures further contribute to raising β_o values because the crystals force coplanarity of the biphenyl moiety ($\gamma \approx 0°$ in **Xb**) in all cases and increase the azine twist angle ($\tau \approx 140°$ in **XaH**) for the true racemates.

The focal point of our research has been the optimization of SHG generation by crystalline solids of the pure NLO materials as the result of dipole-parallel aligned supramolecular structures of D–A substituted organics and dipeptides.[52,53] We computed molecular β_o values to compare series of NLO materials and, in a few cases only, we characterize the SHG activity in the crystal.[22,52] With the availability of several representatives of several series of ferroelectric organics, it is now possible to

Chem. Eur. J. **2024**, e202400182 (8 of 10)

© 2024 Wiley-VCH GmbH

establish for the very first time experimental structure-function relations for the NLO activity of ferroelectric molecular crystals and we aim to perform maker-fringe studies.

Experimental Section

General Synthesis of 4′-(4″-Methoxyphenyl)acetophenone 4-Haloacetophenone Azines, 1–4

The synthesis of the (MeO—Ph, Y)-azines couples two acetophenones, the 4′-methoxy-4-acetylbiphenyl that was prepared by the Suzuki Pd catalyzed cross coupling reaction.[49] The other acetophenones are commercially available. The starting materials are then reacted together using phosphorohydrazidate chemistry developed by Zwierzak based on Wadsworth-Emmons type chemistry (Figure 5, ESI†).[50]

The coupling reactions of the phosphinyl hydrazone and acetophenone were carried out in a dry nitrogen atmosphere glovebox and flame dried glassware. The 4-methoxyphenyl boronic acid and the acetophenones were purified by recrystallization. Benzene, methylene chloride, and 1,4-dioxane were distilled over CaH_2 to remove water. THF was distilled over sodium-benzophenone and anhydrous DME was purchased and used as is. Chromatographic separations used ultra-pure silica gel (230–400 mesh). ^{1}H NMR was recorded on a Bruker ARX-250 (250 MHz), DRX-300 (300 MHz) spectrometer and are reported in ppm with tetramethyl silane (TMS) used as an internal standard. ^{13}C NMR spectra were recorded on a Bruker ARX-250 (62.5 MHz), DRX-300 (75 MHz) and DRX-500 (125 MHz) spectrometer with complete proton decoupling. Chemical shifts are reported in ppm with TMS solvent as the internal standard.[51]

The para-substituted acetophenone is added to a flask of distilled benzene. A tenfold molar equivalent of diethyl phosphorohydrazidate is added to the reaction mixture and then refluxed for 4 hours with the azeotropic removal of water. The remaining solvent is then removed under vacuo. The product is then purified by column chromatography on silica gel by 50:50 CH_2Cl_2:EtOAc. DME (5 ml) is added to an oven dried round bottom flask equipped with a magnetic stir bar. NaH (2.1 mmol) is added to the DME and then added drop wise to a solution of DME (10 ml) and phosphinyl hydrazone (1.33 mmol) prepared in previous step. The reaction was then stirred for about 20 min with the production of hydrogen gas. After the evolution of hydrogen gas ceased, a solution of DME (5 ml) and 4-acetylbiphenyl (1.33 mmol) was added drop wise and stirred for 2–4 hours. The DME was removed under vacuo and then dissolved in CH_2Cl_2 and multiple washes with distilled water until neutral in a separation funnel and then dried with $MgSO_4$. The reaction was then purified by two silica gel columns. First to collect unreacted phosphinyl hydrazone with 50:50 CH_2Cl_2:EtOAc and the second one to purify the compound using 8:1:1 Hex:CH_2Cl_2:EtOAc.

Crystal growth of the compounds utilized two common methods: **1**, **2**, and **4** were crystallized by slow evaporation of chloroform, **3** was crystallized using the slow diffusion of hexane into chloroform. The crystals formed were of X-ray quality and used for X-ray crystallography.

Experimental Data: 4′-(4″-Methoxyphenyl)acetophenone 4-Fluoroacetophenone Azine (1)

Light yellow crystalline solid; ^{1}H NMR (500 MHz, CDCl₃): δ 7.97 (d, 2H), 7.92 (qt, 2H), 7.62 (d, 2H), 7.58 (d, 2H), 7.11 (overlapping doublets, 2H), 3.87 (s, 3H), 2.36 (s, 3H), 2.34 (s, 3H); ^{13}C NMR (125 MHz, CDCl₃): δ 159.4, 158.0, 157.0, 142.0, 136.6, 133.0, 128.6, 128.5, 128.1, 127.0, 126.5, 115.4, 115.2, 114.3, 55.4, 15.0, 15.0.

4′-(4″-methoxyphenyl)acetophenone 4-chloroacetophenone azine (**2**): Light yellow crystalline solid; ^{1}H NMR (250 MHz, CDCl₃): δ 7.85 (d, 2H), 7.76 (d, 2H), 7.49 (overlapping doublets, 4H), 7.28 (d, 2H J = 8.53 Hz), 6.88 (d, 2H), 3.74 (s, 3H), 2.22 (s, 3H), 2.21 (s, 3H); ^{13}C NMR (75 MHz, CDCl3): δ 159.5, 158.0, 142.1, 136.9, 136.6, 135.7, 133.0, 128.5, 128.1, 127.9, 127.1, 126.5, 114.3, 55.4, 15.0, 14.9.

4′-(4″-methoxyphenyl)acetophenone 4-bromoacetophenone azine (**3**): Light yellow crystalline solid; ^{1}H NMR (250 MHz, CDCl₃): δ 7.96 (d, 2H), 7.80 (d, 2H), 7.62 (d, 2H), 7.58 (d, 2H), 7.56 (d, 2H), 7.00 (d, 2H), 3.87(s, 3H), 2.35 (s, 3H), 2.32 (s, 3H); ^{13}C NMR (62.5 MHz, CDCl₃): δ 159.5, 158.0, 157.0, 142.1, 137.3, 136.6, 132.9, 131.5, 128.2, 128.1, 127.1, 126.5, 124.0, 114.3, 55.4, 15.0, 14.9.

4′-(4″-methoxyphenyl)acetophenone 4-iodoacetophenone azine (**4**): Light yellow crystalline solid; ^{1}H NMR (250 MHz, CDCl₃): δ 7.96 (d, 2H), 7.80 (d, 2H), 7.62 (d, 2H), 7.58 (d, 2H), 7.56 (d, 2H), 3.87(s, 3H), 2.35 (s, 3H), 2.32 (s, 3H); ^{13}C NMR (62.5 MHz, CDCl₃): δ 159.5, 158.0, 157.0, 142.1, 137.3, 136.6, 132.9, 131.5, 128.2, 128.1, 127.1, 126.5, 124.0, 114.3, 55.4, 15.0, 14.9.

Author Contributions

H. Bhoday: formal analysis, computational analysis, methodology, visualization, and writing; N. Knotts: synthesis, crystallization, and characterization; R. Glaser: conceptualization, formal analysis, methodology, visualization, funding acquisition, project administration, resources, supervision and mentoring, and writing.

Conflict of Interests

The authors declare no conflict of interest.

Data Availability Statement

The data generated in this study are provided in the Supplementary Information (ORTEP diagrams, Cartesian coordinates of the optimized structures, Hirshfeld surfaces and 2-D fingerprint plots, Synthetic route) and this published article. X-ray structural data of compound **1** (CCDC 2205422), **2** (CCDC 2205421), **3** (CCDC 2205420), and **4** (CCDC 2205423) are available free of charge from the Cambridge Crystallographic Data Center via www.ccdc.cam.ac.uk/data_request/cif.

[1] Y. Zheng, P. Cheng, X. Qian, J. Guan, R. Shi, M. Xin, J. Xu, X. Bu, *Mater. Chem. Front.* **2023**, *7*, 698–704.

[2] R. Akiyoshia, S. Hayami, *Chem. Commun.* **2022**, *58*, 8309–8321.

[3] X. Liu, Z. Yang, D. Wang, H. Cao, *Crystals* **2016**, *6*, 1–19.

[4] T. Tong, W. Zhang, Z. Yang, S. Pan, *Angew. Chem. Int. Ed.* **2020**, *60*, 1332–1338.

[5] S. J. Kim, B. J. Kang, U. Puc, W. T. Kim, M. Jazbinsek, F. Rotermund, O. P. Kwon, *Adv. Opt. Mater.* **2021**, *9*, 1–46.

[6] T. Ghosh, M. Mondal, R. K. Vijayaraghavan, *Mater. Chem. Front.* **2022**, *6*, 297–305.

[7] L. Mencaroni, C. Bonaccorso, V. Botti, B. Carlotti, G. Consiglio, F. Elisei, C. G. Fortuna, A. Spalletti, A. Cesaretti, *Dyes Pigm.* **2021**, *194*, 1–12.

[8] R. Akiyoshia, S. Hayami, *Chem. Commun.* **2022**, *58*, 8309–8321.

[9] D. Steiger, C. Ahlbrandt, R. Glaser, *J. Phys. Chem. B* **1998**, *102*, 4257–4260.

[10] R. Glaser, *Acc. Chem. Res.* **2007**, *40*, 9–17.

[11] M. Lewis, Z. Wu, R. Glaser, In *ACS Symposium Series, Vol. 798* (Eds.: R. Glaser, P. Kaszynski), American Chemical Society, Washington, D. C., **2001**, pp. 97–111.

[12] M. Lewis, R. Glaser, *J. Org. Chem.* **2002**, *67*, 1441–1447.

[13] M. Lewis, C. L. Barnes, R. Glaser, *Acta Crystallogr. Sect. C* **2000**, *56*, 393–396.

[14] G. S. Chen, J. K. Wilbur, C. L. Barnes, R. Glaser, *J. Chem. Soc. Perkin Trans. 2* **1995**, 2311–2317.

[15] M. Lewis, C. L. Barnes, R. Glaser, *J. Chem. Crystallogr.* **2000**, *30*, 489–496.

[16] H. Bhoday, M. Lewis, S. P. Kelley, R. Glaser, *ChemPlusChem* **2022**, *87*, e202200224, 1–7.

[17] H. Bhoday, S. P. Kelley, R. Glaser, *CrystEngComm* **2023**, *25*, 2175–2180.

[18] H. Bhoday, S. P. Kelley, R. Glaser, *CSD Communication* **2021**, CCDC 2103130.

[19] M. Lewis, H. Bhoday, C. L. Barnes, S. P. Kelley, R. Glaser, *CSD Communication* **2020**, CCDC 2017223.

[20] M. Lewis, H. Bhoday, A. Choudhury, S. P. Kelley, R. Glaser, *CSD Communication* **2020**, CCDC 2014691.

[21] M. Lewis, H. Bhoday, C. L. Barnes, S. P. Kelley, A. Choudhury, R. Glaser, *CSD Communication* **2020**, CCDC 2017222.

[22] R. Glaser, N. Knotts, P. Yu, L. Li, M. Chandrasekhar, C. Martin, C. L. Barnes, *Dalton Trans.* **2006**, *23*, 2891–2899.

[23] N. Knotts, R. Glaser, C. L. Barnes, S. P. Kelley, *CSD Communication* **2020**, CCDC 2040896.

[24] N. Knotts, R. Glaser, C. L. Barnes, S. P. Kelley, *CSD Communication* **2020**, CCDC 2040898.

[25] N. Knotts, R. Glaser, C. L. Barnes, S. P. Kelley, *CSD Communication* **2020**, CCDC 2040895.

[26] H. Bhoday, S. P. Kelley, R. Glaser, *CSD Communication* **2022**, CCDC 2202941.

[27] C. L. Barnes, S. P. Kelley, N. Knotts, R. Glaser, *CSD Communication* **2018**, CCDC 1843924.

[28] K. Yang, N. Corretjer, S. Gadban, J. Ratchford, S. P. Kelley, R. Glaser, *CSD Communication* **2019**, CCDC 1955371.

[29] S. P. Kelley, C. L. Barnes, J. Ratchford, R. Glaser, *CSD Communication* **2018**, CCDC 1843925.

[30] C. L. Barnes, S. P. Kelley, M. Lewis, R. Glaser, *CSD Communication* **2018**, CCDC 1838226.

[31] N. Knotts, R. Glaser, C. L. Barnes, S. P. Kelley, *CSD Communication* **2020**, CCDC 2040897.

[32] V. Cozan, M. Avadanei, S. Shova, M. F. Zaltariov, *Liq. Cryst.* **2018**, *46*, 492–501.

[33] R. Glaser, G. S. Chen, C. L. Barnes, *J. Org. Chem.* **1994**, *58*, 7446–7455.

[34] R. Glaser, G. S. Chen, M. Anthamatten, C. L. Barnes, *J. Org. Chem.* **1994**, *59*, 4336–4340.

[35] J. Grzegorzek, Z. Mielke, A. Filarowski, *J. Mol. Struct.* **2010**, *976*, 371–376.

[36] H. Bhoday, K. Yang, S. P. Kelley, R. Glaser, *CrystEngComm* **2023**, *25*, 4638–4657.

[37] N. Knotts, C. L. Barnes, S. P. Kelley, R. Glaser, *CSD Communication* **2022**, CCDC 2205422.

[38] N. Knotts, C. L. Barnes, S. P. Kelley, R. Glaser, *CSD Communication* **2022**, CCDC 2205421.

[39] N. Knotts, C. L. Barnes, S. P. Kelley, R. Glaser, *CSD Communication* **2022**, CCDC 2205420.

[40] N. Knotts, C. L. Barnes, S. P. Kelley, R. Glaser, *CSD Communication* **2022**, CCDC 2205423.

[41] G. P. Charbonneau, Y. Delugeard, *Acta Crystallogr. Sect. B* **1976**, *32*, 1420–1423.

[42] A. Almenningen, O. Bastainsen, L. Fernholt, B. N. Cycin, S. J. Cycin, S. J. Samdal, *J. Mol. Struct.* **1985**, *128*, 59–76.

[43] F. Grein, *J. Phys. Chem.* **2002**, *106*, 3823.

[44] R. Glaser, N. Knotts, Z. Wu, C. L. Barnes, *Cryst. Growth Des.* **2006**, *6*, 235–240.

[45] L. Fábián, C. P. Brock, *Acta Crystallogr. Sect. B* **2010**, *66*, 94–103.

[46] Gaussian 16, Revision C.01, M. J. Frisch, G. W. Trucks, H. B. Schlegel, G. E. Scuseria, M. A. Robb, J. R. Cheeseman, G. Scalmani, V. Barone, G. A. Petersson, H. Nakatsuji, X. Li, M. Caricato, A. V. Marenich, J. Bloino, B. G. Janesko, R. Gomperts, B. Mennucci, H. P. Hratchian, J. V. Ortiz, A. F. Izmaylov, J. L. Sonnenberg, D. Williams-Young, F. Ding, F. Lipparini, F. Egidi, J. Goings, B. Peng, A. Petrone, T. Henderson, D. Ranasinghe, V. G. Zakrzewski, J. Gao, N. Rega, G. Zheng, W. Liang, M. Hada, M. Ehara, K. Toyota, R. Fukuda, J. Hasegawa, M. Ishida, T. Nakajima, Y. Honda, O. Kitao, H. Nakai, T. Vreven, K. Throssell, J. A. Montgomery, Jr., J. E. Peralta, F. Ogliaro, M. J. Bearpark, J. J. Heyd, E. N. Brothers, K. N. Kudin, V. N. Staroverov, T. A. Keith, R. Kobayashi, J. Normand, K. Raghavachari, A. P. Rendell, J. C. Burant, S. S. Iyengar, J. Tomasi, M. Cossi, J. M. Millam, M. Klene, C. Adamo, R. Cammi, J. W. Ochterski, R. L. Martin, K. Morokuma, O. Farkas, J. B. Foresman, D. J. Fox, Gaussian, Inc., Wallingford CT, **2016**.

[47] H. Bhoday, R. Glaser, *to be published*.

[48] J. C. Cole, C. R. Groom, M. G. Read, I. Giangreco, P. McCabe, A. M. Reilly, G. P. Shields, *Acta Crystallogr.* **2016**, *B72*, 530–541.

[49] A. F. Littke, C. Dai, G. C. Fu, *J. Am. Chem. Soc.* **2000**, *122*, 4020–4028.

[50] A. Zwierzak, A. Sulewska, *Synthesis* **1976**, 835–837.

[51] N. Knotts, PhD Thesis, University of Missouri (USA), **2005**.

[52] S. Khanra, S. Vassiliades, W. Alves, K. Yang, R. Glaser, K. Ghosh, P. Bhattacharya, P. Yu, S. Guha, *AIP Adv.* **2019**, *9*, 115202–115206.

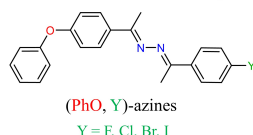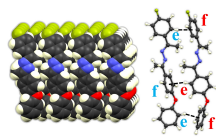[53] K. Yang, F. Gallazzi, C. Arens, R. Glaser, *ACS Omega* **2022**, *7*, 42629–42643.
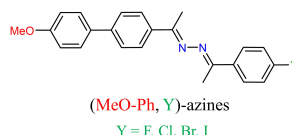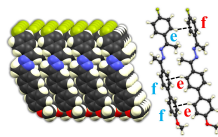
RESEARCH ARTICLE

- Double T-contacts
  ⇒ PBAM formation
- β_o values ≈ 15 - 20 • 10^{-30} esu
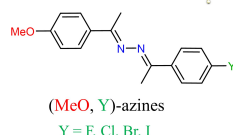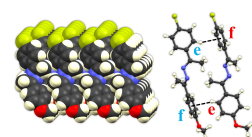
- Triple T-contacts
  ⇒ Higher PBAM stability
  ⇒ Faster crystallization
- β_o values ≈ 15 - 20 • 10^{-30} esu

- Stronger Triple T-contacts
  ⇒ Highest PBAM stability
  ⇒ Fastest crystallization
- β_o values ≈ 45 - 60 • 10^{-30} esu
  ⇒ Extended conjugation

(MeO, Y)-azines
Y = F, Cl, Br, I

(PhO, Y)-azines
Y = F, Cl, Br, I

(MeO-Ph, Y)-azines
Y = F, Cl, Br, I

Increasing crystal lattice stabilization and NLO performance

H. Bhoday, Dr. N. Knotts, Dr. R. Glaser*

1 – 11

Perfect Polar Alignment of Parallel Beloamphiphile Layers: Improved Structural Design Bias Realized in Ferroelectric Crystals of the Novel "Methoxyphenyl Series of Acetophenone Azines"

The achievement of perfect polar dipole alignment in ferroelectric lattices of organic non-linear optical (NLO) materials demonstrates the potential for crystal engineering by rational design to craft materials with advanced optical performance. The methoxyphenyl series of acetophenone azines feature polar stacking of parallel beloamphiphile monolayers (PBAMs). These third-generation chromophores feature superior triple T-contacts and improved crystal growth, and they excel because of their enhanced NLO properties.